

Path Query Data Structures in Practice

Meng He

Faculty of Computer Science, Dalhousie University, Canada
mhe@cs.dal.ca

Serikzhan Kazi

Faculty of Computer Science, Dalhousie University, Canada
skazi@dal.ca

Abstract

Let us be given an ordinal tree, such that each node of it has a certain associated weight. We design, implement, and evaluate space- and time-performance of data structures to answer online *path queries* on such a tree: path counting, path reporting, and path median queries. These query problems generalize the well-known problems of $2d$ orthogonal range counting and reporting in planar point sets, as well as the range median query problem in arrays, to tree structured data. We propose practical realizations of the latest theoretical results in path queries. Our data structures, whose components include tree extraction, heavy-path decomposition, and wavelet trees, are implemented in both succinct and plain pointer-based form. Our succinct data structures are further specialized into entropy-compressed and plain forms. Through a set of experiments on large datasets, we show that succinct data structures for path queries present a viable alternative to standard pointer-based realizations in practical scenarios. We compare the performance of our data structures to naïve approaches that encode the tree in plain pointer-based form and do not preprocess it to speedup the queries, but rather compute the answer by explicitly traversing the query path and checking the nodes. Our succinct data structures are several times faster in path median queries, and perform comparably in path counting and path reporting queries, while being several times more space-efficient, than such naïve approaches. Plain pointer-based realizations of our data structures, requiring a few times more space than the naïve structures, yield a 30-100-times speedup over them. In addition, our succinct data structures provide more functionality within the little space they use than their plain pointer-based counterparts.

2012 ACM Subject Classification Information systems → Data structures

Keywords and phrases path queries range queries algorithms data structures experiments

Digital Object Identifier 10.4230/LIPIcs...

Funding This work was supported by NSERC of Canada.

1 Introduction

Let T be an ordinal tree on n nodes, with each node being associated with a *weight* over an alphabet $[\sigma]$.¹ *Path counting* (*path reporting*) query counts (reports) the nodes on the query path with weights falling inside the query weight range. These queries generalize traditional $2d$ orthogonal counting and reporting queries in $2d$ point sets, to the case when one dimension is replaced by tree topology.

Apart from theoretical appeal, queries on tree topologies reflect the needs of efficient information retrieval from hierarchical data, which are gaining ground in established domains such as RDBMS [27, 12, 6]. The computational challenge owes to the expected height of T being $\sqrt{2\pi n} = \Theta(\sqrt{n})$ [76], which calls for the development of methods beyond explicitly scanning the query path.

Formally, queries present us with a pair of vertices $x, y \in T$, and an interval Q . With $P_{x,y}$ henceforth denoting the path from x to y in the tree T , and $\mathbf{w}(z)\mathbb{N}$ being the weight of a node $z \in T$, the goal is to preprocess the tree T for the following types of queries:

- *Path Counting*: return $|\{z \in P_{x,y} \mid \mathbf{w}(z) \in Q\}|$.

¹ we set $[n] \triangleq \{1, 2, \dots, n\}$.



© Meng He and Serikzhan Kazi;
licensed under Creative Commons License CC-BY



Leibniz International Proceedings in Informatics
Schloss Dagstuhl – Leibniz-Zentrum für Informatik, Dagstuhl Publishing, Germany

- *Path Reporting*: enumerate $\{z \in P_{x,y} \mid \mathbf{w}(z) \in Q\}$.
- *Path Selection*: return the k^{th} weight in the sorted list of weights of $P_{x,y}$; k is given at query time.

Path queries is a widely-researched topic in computer science community [17, 30, 46, 57, 36, 51, 28, 47]. We refer the reader to e.g. [51, 47] for an overview of previous work on the path counting and reporting problems.

Krizanc et al. [57] were the first to introduce path median query problem in trees, and gave an $\mathcal{O}(\lg n)$ query-time data structure with the space cost of $\mathcal{O}(n \lg^2 n)$ words. They also gave an $\mathcal{O}(n \log_b n)$ words data structure to answer range median queries in trees in time $\mathcal{O}(b \lg^3 n / \lg b)$, for any fixed $1 \leq b \leq n$. These running times were later improved by [49] to be $\mathcal{O}(\lg \sigma)$, while occupying $\Theta(n \lg n)$ bits of space. Patil et al. [73] presented an $\mathcal{O}(\lg n \cdot \lg \sigma)$ query-time data structure, with space occupancy of $6n + n \lg \sigma + \mathcal{O}(n \lg \sigma)$ bits. Therein, the tree structure and the weights distribution are decoupled and delegated to respectively *heavy-path decomposition* [78] and *wavelet trees* [64]. He et al. [51] further employed *tree extraction* to partition the tree simultaneously along the weights and tree structure dimensions, to achieve $\mathcal{O}(\lg \sigma / \lg \lg \sigma)$ query time and $nH(W_T) + \mathcal{O}(n \lg \sigma)$ bits of space, where $H(W_T)$ is the zeroth-order entropy of the set of weights W_T of the tree.

Despite the vast body of work, little is known on the practical performance of the data structures for path queries, with empirical studies on weighted trees definitely lacking, and existing related experiments being limited to navigation in unlabeled trees only [18], or to very specific domains [15, 66]. By contrast, the traditional orthogonal range queries have enjoyed commensurate attention from both theoretical (see e.g. [54, 68, 29, 25, 69]) and empirical (see e.g. [19, 24, 52]) perspectives. We therefore contribute to remedying this imbalance.

1.1 Our Results

In this article, we provide an experimental study of data structures for path queries. The types of queries we consider are path median (PM), path counting (PC), and path reporting (PR). The theoretical foundation of our work are the data structures and algorithms developed in [49, 73, 50, 51]. The succinct data structure by He et al. [51] is optimal both in space and time in the RAM model. However, it builds on components that are likely to be cumbersome in practice. We therefore present a practical compact implementation of this data structure (henceforth referred to as `ext`) that uses $3 \lg \sigma$ bits per node as opposed to the original H_0 bits per node in [51]. Our implementation achieves the query time of $\mathcal{O}(\lg \sigma)$ for PM and PC queries, and $\mathcal{O}((1 + \kappa) \lg \sigma)$ time for PR, where κ henceforth denotes output size; all these bounds are optimal in the pointer-machine model. Further, we present the exact implementation of the data structure (henceforth `whp`) by Patil et al. [73]. The theoretical guarantees of `whp` are $6n + n \lg \sigma + \mathcal{O}(n \lg \sigma)$ bits of space, with $\mathcal{O}(\lg n \lg \sigma)$ and $\mathcal{O}(\lg n \lg \sigma + (1 + \kappa) \lg \sigma)$ query times for respectively PM/PC and PR. Although `whp` is optimal neither in space nor in time, it turns out to be competitive with `ext` on the practical datasets we use. Further, we evaluate time- and space-impact of succinctness by realizing plain pointer-based versions of `ext` and `whp`. We show that succinct `ext` and `whp` offer an attractive alternative for their fast but space-consuming counterparts, with query-time slowdown of 30-40 times yet commensurate savings in space.

1.2 Outline of Article

The rest of the article is organized as follows. In the next section, we briefly introduce the notation and the main algorithmic techniques at the core of our data structures. Then, in Section 3, we show how to represent our data structures in compact form while supporting fast navigation and queries, using results from succinct data structures, as building blocks. In it, we give the details of the $6n + n \lg \sigma + \mathcal{O}(n \lg \sigma)$ and $3n \lg \sigma + \mathcal{O}(n \lg \sigma)$ bits-of-space representations for respectively `whp` and

Symbol	Description
pointer-based	nv Naïve data structure in Section 2.2
	nv^L Naïve data structure in Section 2.2, augmented with $\mathcal{O}(1)$ query-time LCA of [22]
	ext^\dagger Tree extraction of [51] in Section 2.1
	whp^\dagger Wavelet tree- and heavy-path decomposition-based solution of [73] in Section 3.
succinct	nv^c Naïve data structure of Section 2.2, using <code>bp_support_gg</code> of <code>sds1-lite</code>
	whp^p Succinct version of whp , with uncompressed bitmaps
	whp^c Succinct version of whp , with compressed bitmaps
	ext^p The $3\lg\sigma$ -bit scheme for tree extraction of Section 3.2, with uncompressed bitmaps
	ext^c The $3\lg\sigma$ -bit scheme for tree extraction of Section 3.2, with compressed bitmaps

Table 1 – The implemented data structures and the abbreviations used to refer to them. When presenting the data in tables, we sometimes refer to whp^p and whp^c as respectively $whp(p)$ and $whp(c)$, to indicate that plain and compressed bitmaps are used. Analogously for ext^p and ext^c .

ext . Central to the section is the approach to support constant-time 0/1-ancestor queries, which are tree analogs of the traditional rank queries for sequences. The proposed approach saves one bit per node when compared to straightforward approaches such as multi-parentheses sequences [65], and is of independent interest. In Section 4.1, we measure practical performance of the designed data structures, in terms of space occupied, average query time for the types of queries we consider, and peak memory consumption during construction, on practical datasets hailing from various sources such as GIS and DIMACS. Finally, in Section 5 we conclude our study with key observations and discuss some open problems.

For ease of reference, we outline the data structures implemented in Table 1.

2 Preliminaries

2.1 Background

Notation adopted is rather standard. The i^{th} node visited during a preorder traversal of the given tree T is said to have *preorder rank* i . We identify the node by its preorder rank. For a node $x \in T$, its set of ancestors, denoted as $\mathcal{A}(x)$, includes x itself; $\mathcal{A}(x) \setminus \{x\}$ is then the set of *proper ancestors* of x . Given two nodes $x, y \in T$, where $y \in \mathcal{A}(x)$, we set $A_{x,y} \triangleq P_{x,y} \setminus \{y\}$. A path $P_{x,y}$ can then be written as $A_{x,z} \sqcup \{z\} \sqcup A_{y,z}$, where $z = LCA(x, y)$. A node (resp. ancestor) with label α is called an α -node (resp. α -ancestor). The primitives `rank`/`select`/`access` are defined in a standard way, i.e. `rank1(B, i)` is the number of 1-bits in positions less than i , `select1(B, j)` returns the position of the j^{th} 1-bit, and `access(B, i)` returns the bit at the i^{th} position, all with respect to a given bitmap B , which is omitted when the context is clear.

Compact representations of ordinal trees is a well-researched area, mainstream methodologies including *balanced parentheses* (BP) [53, 41, 62, 31, 77, 58, 61], *depth-first unary degree sequence* (DFUDS) [23, 42, 55], *level-order unary degree sequence* (LOUDS) [53, 35], and *tree covering* [42, 50, 37]. Of these, BP-based representations “combine good time- and space-performance with rich functionality” (Arroyuelo et al. [18]), and we use BP in our solutions. In Appendix A given is an overview of BP representation of ordinal trees. Formally, the central result on succinct representation of ordinal trees that is used in our study, is summarized in

► **Lemma 1** ([51, 48]). *If T is an ordinal tree on n nodes, each having a label drawn from $[\sigma]$, where $\sigma = \mathcal{O}(\lg^\varepsilon n)$ for some constant $0 < \varepsilon < 1$, then T can be represented in $n(\lg\sigma + 2) + \mathcal{O}(n)$ bits of*

XX:4 Path Query Data Structures

space to support the following operations in $\mathcal{O}(1)$ time, for any node $x \in T$: $\text{depth}(T, x)$, the number of ancestors of x ; $\text{LCA}(T, x, y)$, the lowest common ancestors of nodes $x, y \in T$; $\text{pre_rank}_\alpha(T, x)$, the number of α -nodes that precede x in preorder; $\text{pre_select}_\alpha(T, i)$, the i -th α -node in preorder.

Lemma 1 contains within two important special cases: of unlabeled trees ($\sigma \equiv 1$) and of 0/1-labeled trees ($\sigma \equiv 2$), effectively stating that the mentioned $\mathcal{O}(1)$ -time operations can be supported in respectively $2n + \mathcal{O}(n)$ [48] and $3n + \mathcal{O}(n)$ bits of space.

Tree extraction [51] selects a subset X of nodes while maintaining the underlying hierarchical relationship among the nodes in X . Given a subset X of tree nodes called *extracted nodes*, an *extracted tree* T_X can be obtained from the original tree T through the following procedure. Let $v \notin X$ be an arbitrary node. The node v and all its incident edges in T are removed from T , thereby exposing the parent p of v and v 's children, v_1, v_2, \dots, v_k . Then the nodes v_1, v_2, \dots, v_k (in this order) become new children of p , occupying the contiguous segment of positions starting from the (old) position of v . After thus removing all the nodes $v \notin X$, we have $T_X \equiv F_X$, if the forest F_X obtained is a tree; otherwise, a dummy root r holds the roots of the trees in F_X (in the original left-to-right order) as its children. (The symmetry between X and $\bar{X} = V \setminus X$ brings about the *complement* $T_{\bar{X}}$ of the extracted tree T_X .) An original node $x \in X$ of T and its copy, x' , in T_X are said to *correspond* to each other; it is also said that x' is the T_X -view of x , and x is the T -source of x' . The T_X -view of a node $y \in T$ (y is not necessarily in X) is generally defined to be the node $y' \in T_X$ corresponding to the lowest node in $\mathcal{A}(y) \cap X$. Figure 1 gives an example of an extracted tree, its complement, views and sources.

Heavy-path decomposition [78] imposes a structure on trees. In HPD, for each non-leaf node, defined is a *heavy child* as the child whose subtree has the maximum cardinality. HPD decomposes the tree into a set of disjoint *chains*, in each of which a node is followed by its heavy child. The crucial property is that any root-to-leaf path in the tree encounters $\mathcal{O}(\lg n)$ distinct chains. In Figure 2a, there are 5 chains overall: $1 \rightarrow 2 \rightarrow 3 \rightarrow 5$, three singleton chains 4, 6, and 10, and one more chain $7 \rightarrow 8 \rightarrow 9$. Chain's *head* is the node of the chain that is closest to the root. The heads of these chains are thus respectively 1, 4, 6, 10, and 7. A chain's tail is therefore a leaf, and chain's head is either (i) the root of the tree, or (ii) a non-heavy child of its parent (such as e.g. node 7 and its parent node 1 in Figure 2a). Chain being an array-like structure, one taps into the plethora of preprocessing methods for linear structures. Since each path in a tree can be decomposed into $m = \mathcal{O}(\lg n)$ disjoint sub-paths, the entire query is distributed across m disjoint sub-queries over the already-preprocessed chains.

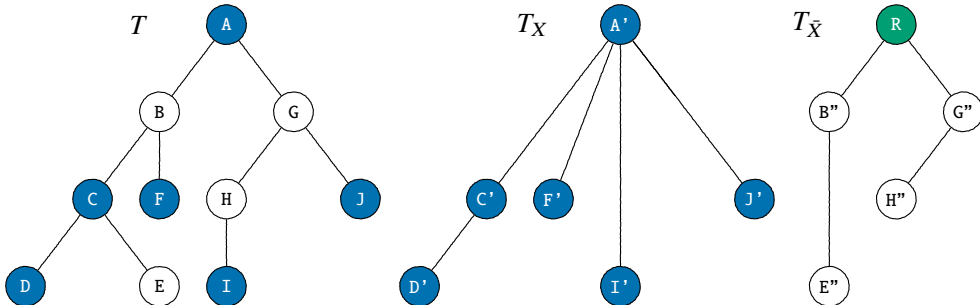


Fig. 1. Tree extraction. Original tree (left), extracted tree T_X (middle), and extraction of the complement of X , tree $T_{\bar{X}}$ (right). The blue shaded nodes in T form the set X . In the tree T_X , node C' corresponds to node C in the original tree T , and node C' in the extracted tree T_X is the T_X -view of nodes C and E in the original tree T . Finally, node C in T is the T -source of the node C' in T_X . Extraction of the complement, $T_{\bar{X}}$, demonstrates the case of adding a dummy root R .

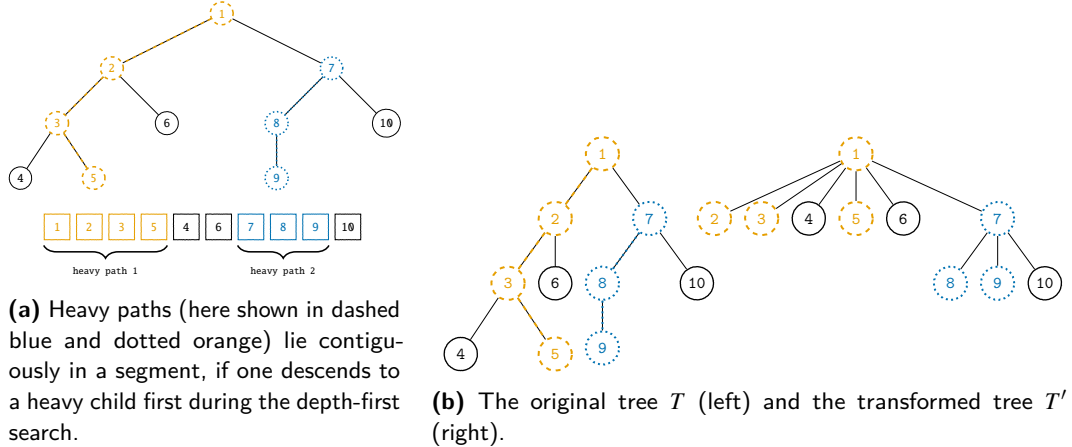


Fig. 2. Heavy-path decomposition of a tree (left) and transformation thereof (right) for compact encoding.

2.2 Approaches

Having introduced our tools, we next give some base aspects of the implemented data structures and underlying algorithms for solving PM, PC, and PR. Since the generic approach for finding order statistics is well-known [34], we only outline the variations thereof pertaining to whp and ext. See Appendix D for details.

Wavelet tree- and heavy-path decomposition-based solution exploits the property that, if during a depth-first search one always descends to the heavy child first, a heavy path will lie contiguously in the resulting preorder list [73] (see Figure 2a). Then, the corresponding preorder weight sequence (PWS) is queried with $\mathcal{O}(\lg n)$ simultaneous (i) range quantile [39] queries (PM); or (ii) orthogonal range $2d$ queries (PC and PR).

Tree extraction-based solution proceeds by applying the extraction procedure recursively to the extracted trees, by systematically halving the weight-set associated with the current tree. One starts with the original tree T weighted over $[\sigma]$, and extracts two trees $T_0 = T_{1,m}$ and $T_1 = T_{m+1,\sigma}$, respectively associated with the intervals $I_0 = [1, m]$ and $I_1 = [m+1, \sigma]$, where $m = \frac{1+\sigma}{2}$. Then both T_0 and T_1 are subject to the same procedure, stopping only when the current tree is weight-homogeneous. We refer to the tree we have started with as the *outermost* tree.

From the perspective of path queries, the key insight of tree extraction is that the number of nodes m with weights from I_0 on the path from u to v equals [51]

$$m = \text{depth}_0(u_0) + \text{depth}_0(v_0) - 2 \cdot \text{depth}_0(z_0) + 1_{w(z) \in I_0} \quad (*)$$

where $\text{depth}_0(\cdot)$ is the depth function in T_0 , z is the LCA of u and v , u_0, v_0, z_0 are the views of u, v , and z in T_0 , and 1_{pred} is 1 if predicate $pred$ is TRUE, and 0 otherwise. It is clear that the key step is for a given node x , how to efficiently find its 0/1-ancestor, which is analogous to a rank-query when descending down the wavelet tree. This question is addressed in Section 3. Resolving queries themselves is consigned to Appendix D in the interests of brevity, and the reader is referred to [49, 51] for details.

Naïve structures represent pointer-based tree topologies via *forward-star* [16] method. For succinct storage of tree topologies (nv^c), we use BP. A query with nodes u and v as arguments is resolved by explicitly traversing the path from u to v . In PM, we subsequently call standard selection algorithm [63] (implemented in `nth_element()` of C++) over the array of collected weights. Depths and parent pointers, explicitly stored at each node, guide in upwards traversal from u and v to their common ancestor. Depths guard against traversing the entire way up to the root.

3 Compact Representations

3.1 Encoding for whp

We examine the anatomy of HPD for the exposition of Patil et al. [73]’s compact encoding thereof. If x is the head of a chain ϕ , all the nodes in ϕ have a (conceptual) *reference* pointing to x , while x points to itself. A *reference count* of a node x (denoted as rc_x) stands for the number of times a node serves as a reference. Obviously, only heads feature non-zero reference counts – precisely the lengths of their respective chains; for all the other nodes x , one has $rc_x \equiv 0$. The values of rc are stored in unary in a bitmap $B = 10^{rc_1}10^{rc_2}\dots10^{rc_n}$ using $2n + \mathcal{O}(n)$ bits. For Figure 2a, B would be equal to (spaces for readability): 10000 1 1 10 1 10 1000 1 1 10. Then, one has that $rc_x = \text{rank}_0(B, \text{select}_1(B, x+1)) - \text{rank}_0(B, \text{select}_1(B, x))$. For Figure 2a, rc_6 is equal to $\text{rank}_0(\text{select}_1(7)) - \text{rank}_0(\text{select}_1(6)) = \text{rank}_0(13) - \text{rank}_0(11) = 6 - 5 = 1$, as expected, since 6 is the head of a chain of its own. The topology of the original tree T is stored in another $2n + \mathcal{O}(n)$ bits. In addition, we encode the HPD structure in a new tree T' that is obtained from T via the following transformation. All the non-head nodes become leaves and are directly connected to their respective heads; the heads themselves (except the root) become children of the references of their original parents. All these connections are established respecting the preorder ranks of the nodes in the original tree T . Namely, a node farther from the head attaches to it only after the higher-residing nodes of the chain have done so. This transformation preserves the original preorder ranks. In Figure 2b, the head 4 of the singleton chain 4 becomes a child of 1. The chain 1 → 2 → 3 → 5 is transformed so that the nodes 2, 3, and 5 become, in this order, children of the node 1. On T' , operation $\text{ref}(x)$ is supported, which returns the head of chain to which the node x in the original tree belongs.

Having dealt with the topology of the tree and encoded its HPD, we incorporate the weight information. We call C_x the weight-list of x if it collects, in preorder, all the nodes for which x is a reference. As before, a non-head node’s list is empty; a head’s list spells the weights in the relevant chain. Let us set $C = C_1 C_2 \dots C_n$. For Figure 2a, the weights in C would come in this order: 1, 2, 3, 5, 4, 6, 7, 8, 9, 10. It can be seen that in C an arbitrary node x ’s weight resides at position $1 + \text{select}_1(B, \text{ref}(x)) - \text{ref}(x) + \text{depth}(x) - \text{depth}(\text{ref}(x))$ where $\text{depth}(x)$ and $\text{ref}(x)$ are provided by T and T' . Each heavy-path sub-chain is translated into an interval $[l, r]$ over C using this equation, thereby yielding a collection of query intervals, $I_m = \{[l_i, r_i]\}_{i=1}^m$. (Recall that $m = \mathcal{O}(\log n)$ in HPD.) Informally, the superfluous “1”s in B for which there is no corresponding entry in C are skipped over via $\text{select}_1(\text{ref}(x)) - \text{ref}(x)$. The subsequent $\text{depth}(x) - \text{depth}(\text{ref}(x))$ is the offset of x in its reference $\text{ref}(x)$ ’s list. For example, the weight of $x = 3$ is found at position $1 + \text{select}_1(\text{ref}(3)) - \text{ref}(3) + \text{depth}(3) - \text{depth}(1) = 1 + \text{select}_1(1) - 1 + 2 - 0 = 3$. With HPD being a standard technique and extending the range quantile algorithm of [39] to the set of intervals I_m being trivial, we consign further details to Appendix D.

3.2 The $3\lg\sigma$ -bit encoding for ext

Supporting 0/1-ancestors in compact space is one of the main implementation challenges of the technique, as storing the views explicitly is space-expensive. A generic multi-parentheses approach described in [65], would yield a $4n\lg\sigma + 2n + \mathcal{O}(n\lg\sigma)$ -bit encoding of the tree, with $\mathcal{O}(1)$ -time support for 0/1-ancestors. We achieve instead $3n\lg\sigma + \mathcal{O}(n\lg\sigma)$ bits of space as follows. We store $2n + \mathcal{O}(n)$ bits as a regular BP-structure S of the original tree, and mark in a separate length- n bitmap B the *types* (i.e. whether it is a 0 or 1 node) of the n opening parentheses in S . The type of an opening parenthesis at position i in S is thus determined by $\text{access}(B, \text{rank}_1(S, i))$. Given S and B , we find

the $t \in \{0, 1\}$ -ancestor of v with an approach described in [50]. For completeness, we outline in Algorithm 1 how to locate the T_t -view of a node v .

■ **Algorithm 1** – Locate the view of v in T_t in the $3\lg \sigma$ -bit data structure

Require: $t \in \{0, 1\}$

```

function VIEW_OF( $v, t$ )
  if  $B[v] == t$  then ▷  $v$  is a  $t$ -node itself
    return  $B.rank_t(v)$ 
  3:    $\lambda \leftarrow rank_t(B, v)$  ▷ how many  $t$ -nodes precede  $v$ ?
    if  $\lambda == 0$  then
      6:     return null
      u  $\leftarrow select_t(B, \lambda)$  ▷ find the  $\lambda^{th}$   $t$ -node
      if is_ancestor(u, v) then
        9:       return  $B.rank_t(u)$ 
        z  $\leftarrow LCA(u, v)$  ▷  $z$  is LCA of a  $t$ -node  $u$  and a non- $t$ -node  $v$ 
        if z == null or B[z] == t then ▷  $z$  is a  $t$ -node  $\Rightarrow \nexists$   $t$ -ancestor closer to  $v$ 
          12:      return  $B.rank_t(z)$  ▷ or null
           $\lambda \leftarrow rank_t(B, z)$  ▷ how many  $t$ -nodes precede  $z$ ?
          r  $\leftarrow select_t(B, \lambda + 1)$  ▷ the first  $t$ -descendant of  $z$ 
          15:       $z_t \leftarrow rank_t(B, r)$  ▷  $z_t$  is the  $T_t$ -view of  $r$ 
          p  $\leftarrow T_t.parent(z_t)$  ▷  $p$  can be null if  $z_t$  is 0
          return p

```

First, find the number of t -nodes preceding v (line 4). If none exists (line 5), we are done; otherwise, let u be the t -node immediately preceding v (line 7). If u is an ancestor of v , it is the answer (line 9). Otherwise, set z to LCA of u and v . If z is a t -node, or non-existent (because the tree is actually a forest), then return z or `null`, respectively. Otherwise (z exists and not a t -node), in line 14 we find the first t -descendant r of z (it exists because of u). This descendant cannot be a parent of v , since otherwise we would have found it before. We will use it, instead, as the node “closest to being a t -parent” of v . We map this descendant to a node z_t in T_t (line 15). Finally, we find the parent of z_t in T_t (line 16).

The combined space cost of S and B is $3n = 2n + n$ bits, and with the $\lg \sigma$ levels, one obtains a $3n \lg \sigma + \mathcal{O}(n \lg \sigma)$ -bits-of-space data structure. Theoretical running time is $\mathcal{O}(\lg \sigma)$ per query, as all the primitives used are $\mathcal{O}(1)$ -time. This concludes the key ingredients in the compact design of `extP/extC`.

4 Experimental Results

4.1 Experimental Setup

With the implementation details of our data structures given in Appendix B, we focus on design of our experiments. **Platform** used is a 128GiB RAM, Intel(R) Xeon(R) Gold 6234 CPU 3.30GHz server running 4.15.0-54-generic 58-Ubuntu SMP x86_64 kernel. The build is due to clang-8 with `-g, -O2, -std=c++17, mcmodel=large, -NDEBUG` flags. Automated testing, time and space performance measurements are due to `gtest` [4], `g-benchmark` [3], and `malloc_count` [7] libraries, respectively.

Experimental data ideally have inherent tree structure with “naturally-occurring” node-weights.

XX:8 Path Query Data Structures

	num nodes	diameter	σ	$\log \sigma$	H_0	Description	Source
eu.mst.osm	27,024,535	109,251	121,270	16.89	9.52	mst of Europe's map	OSM [71, 9]
eu.mst.dmc	18,010,173	115,920	843,781	19.69	8.93	European road network mst	DIMACS'09 [5]
eu.emst.dem	50,000,000	175,518	5020	12.29	9.95	Euclidean mst for DEM-Europe	SRTM [11]
mrs.emst.dem	30,000,000	164,482	29,367	14.84	13.23	Euclidean mst for DEM-Mars	NASA [8]

Table 2 – Datasets metadata. Weights are over $[\sigma]$, and H_0 is zeroth-order entropy of the multiset of weights. Detailed steps of reproducing the data is given in Appendix C.

	Dataset	nv	nv ^L	whp [†]	ext [†]	nv ^c	ext ^c	ext ^P	whp ^c	whp ^P
space	eu.mst.osm	1.53	3.31	12.31	18.95	0.32	0.44	0.49	0.32	0.36
	eu.mst.dmc	1.02	2.21	9.13	14.36	0.24	0.34	0.39	0.23	0.27
	eu.emst.dem	2.76	6.22	19.92	27.32	0.58	0.73	0.81	0.58	0.65
	mrs.emst.dem	1.63	3.79	12.78	19.08	0.34	0.46	0.51	0.34	0.38
peak/time	eu.mst.osm	1.57/1	3.36/5	12.61/28	30.41/47	0.32/1	1.18/23	1.18/23	4.49/62	4.49/61
	eu.mst.dmc	1.09/1	2.27/4	9.40/19	26.13/37	0.23/1	0.88/18	0.88/18	3.02/42	3.02/42
	eu.emst.dem	2.80/2	6.41/10	20.61/47	31.24/67	0.58/1	2.14/32	2.14/32	8.23/115	8.23/115
	mrs.emst.dem	1.65/1	3.83/5	13.27/30	21.33/46	0.34/1	1.22/22	1.22/22	4.95/69	4.95/69

Table 3 – (upper) Space occupancy of our data structures, in GiB, when loaded into memory; (lower) peak memory usage (\mathbf{m} in GiB) during construction and construction time (t in seconds) shown as \mathbf{m}/t .

While tree topologies per se are abound (e.g. [38, 13]), large instances of trees that are also weighted are not easy to come by. Our datasets originate from Geographical Information Systems (GIS). In Table 2, our datasets are endowed with descriptive handles, and the relevant meta-data is given, with the details consigned to Appendix C.

Query generation for the nodes proceeds by choosing a pair uniformly at random (u.a.r.). In generating range of weights, $[a, b]$, we follow the methodology of [33] by considering three configurations, **large**, **medium**, and **small**: given K , we generate the left bound $a \in [W]$ u.a.r., whereas b is generated u.a.r. from $[a, a + \lceil \frac{W-a}{K} \rceil]$. We set $K = 1, 10$, and 100 for respectively **large**, **medium**, and **small**. To counteract high skew in weight distribution, when generating the weight-range $[a, b]$, we in fact generate a pair from $[n]$ rather than $[\sigma]$ and simply map the positions to the sorted list of weights in the input. This way, the number of nodes covered by the generated weight-range is in (inverse) proportion to K , as evidenced by column κ of Table 5.

4.2 Space Performance

As each of the structures answer all three types of queries, we consider space occupancy, first.

We visualize some typical entries in Table 4 to illustrate the structures clustering along the space/time tradeoffs: nv/nv^L (upper-left corner) are lighter in terms of space, but slow; pointer-based ext[†]/whp[†] are very fast, but space-heavy. Between the two extremes of the spectrum, the succinct structures ext^P, ext^c, whp^P, and whp^c, whose mutual configuration is shown magnified in an inner rectangle, are space-economical and yet offer fast query times, at the same time. The difference between pointer-based ext and whp families is in explicitly storing 0-views for each of the $\Theta(n \lg \sigma)$ nodes that ever occur during tree extraction. In whp, by contrast, rank₀ can be simulated via subtraction of rank₁ – hence the difference in the empirical sizes of the otherwise $\Theta(n \lg \sigma)$ -word data structures. The succinct structures ext and whp are faster than nv/nv^L, but also few times lighter. The entropy-compressed whp^c in practice occupies space equal to information-theoretic minimum, embodied in nv^c, while whp^P/ext^P/ext^c are not too far off, and it is interesting that all do so while supporting efficient queries, and are thus superior to nv^c on all practical aspects. Compared to

Dataset	nv	nv ^L	ext [†]	whp [†]	nv ^c	ext ^c	ext ^c	whp ^c	whp ^p	
median	eu.mst.osm	658	475	4.22	6.10	7078	85.3	51.1	111	51.2
	eu.mst.dmc	566	412	5.16	6.28	6556	84.6	54.8	120	54.7
	eu.emst.dem	710	436	4.44	5.10	9404	106	81.9	96.7	54.9
	mrs.emst.dem	472	298	4.93	4.53	7018	124	97.0	88.3	49.5
counting	eu.mst.osm	238	140	6.88	18.4	3553	247	167	139	56.9
	eu.mst.dmc	204	121	7.31	19.7	3300	253	178	142	57.3
	eu.emst.dem	338	195	5.97	11.5	4835	215	168	105	55.9
	mrs.emst.dem	232	174	5.25	8.40	3614	206	164	91	49.3
medium	eu.mst.osm	244	143	5.47	17.8	3555	213	146	129	54.2
	eu.mst.dmc	209	124	6.94	18.4	3297	224	160	133	56.5
	eu.emst.dem	339	195	4.55	10.0	4840	178	140	100	54.9
	mrs.emst.dem	237	143	5.91	8.74	3613	199	154	89.7	48.9
small	eu.mst.osm	239	139	5.25	15.4	3551	190	132	119	53.9
	eu.mst.dmc	209	123	5.25	18.9	3300	206	148	126	55.2
	eu.emst.dem	347	200	3.92	9.34	4832	154	124	94.9	53.2
	mrs.emst.dem	238	144	4.82	7.41	3615	178	133	84.2	47.6

Table 4 – Average time to answer a query, from a fixed set of 10^6 randomly generated path median and path counting queries, in microseconds. Path counting queries are given in large, medium, and small configurations.

pointer-based solutions (nv/nv^L/whp[†]/ext[†]), it is important to note also that whp^p/whp^c, ext^p/ext^c still allow usual navigational operations on the original tree, whereas the former shed this redundancy, to save space, after preprocessing phase.² Furthermore, Table 3 records peak memory usage (**m**) and construction time (**t**) in seconds, shown as **m/t**. The structures ext^p/ext^c are about three times faster than whp^p/whp^c to build, and use four times less space at peak. This is expected, as whp builds two different structures (heavy-path decomposition of the tree and then wavelet tree.) For pointer-based ext[†] and whp[†] the situation is reversed, timewise because of ext[†] requiring more calls to system memory allocations during construction (although our succinct structures are flattened into heap layout, in ext[†] we opted to store explicit pointers to T_0/T_1 ; this is less of an issue for whp[†], since its very purpose is linearizing the tree).

Overall, the succinct whp^p/whp^c/ext^p/ext^c are all under 1GiB for the large datasets we use, which suggest scalability. When trees are so large as not to fit into main memory, the succinct solutions are the method of choice. For example, we have successfully built ext^c for a randomly generated tree of 1.5 billion nodes.

4.3 Path Median Queries

The lower section of Table 4 records the mean time for a single median query (in microseconds) averaged over a fixed set of 1 million randomly generated queries.

Succinct structures whp^p/whp^c and ext^p/ext^c perform very well on these queries, with a slowdown of at most 20-30 times from their respective pointer-based counterparts. Using compression (`sds1::rrr_vector`) slows down whp almost twice. The fastest structure is whp^p, and for mrs.emst.dem dataset uncompressed ext^p is even slower than compressed whp^c. Overall, though, the families whp and ext seem to perform at the same order of magnitude. This is surprising, as in

² to quote Arroyuelo et al. [18]: “The key advantage is the wide functionality these succinct representations support within this space.”

theory whp should be a factor of $\lg n$ slower. The discrepancy is explained partly by small average number of segments in HPD (averaging 9 ± 2 for our queries). In addition, the search inside whp is trivially optimized to remove the HPD segments that become empty – once removed, they are no longer probed potentially $\mathcal{O}(\lg \sigma)$ times each as we descend down the wavelet tree. More generally, search-related navigation operations, in $\text{ext}^p/\text{ext}^c$ and $\text{whp}^p/\text{whp}^c$, albeit having similar theoretical worst-case guarantees, involve different patterns of using the `rank`/`select` primitives. For one, $\text{whp}^p/\text{whp}^c$ does not call *LCA* during the search – mapping of the search ranges is accomplished by a single `rank` call (see Algorithm 2 in Appendix D). In contrast, $\text{ext}^p/\text{ext}^c$ launches an *LCA* operation at each level of descent (for its own analog of `rank` – the view computation outlined in Algorithm 1). *LCA*, embodied in the `double_enclose()` primitive in BP-parlance, is a non-trivial combination of `rank` and `select` calls. The difference between $\text{ext}^p/\text{ext}^c$ and $\text{whp}^p/\text{whp}^c$ will therefore become apparent in a large enough tree, when the number of segments of HPD is no longer negligible, and the large constants involved in (albeit theoretically constant-time) *LCA* calls is overcome by $\lg n$. (As a sidenote, our experiments also show that on “deep” trees such as depth-first search trees, the number of segments tend to be smaller. In an example of a tree with diameter of 5 million nodes, there were on average only 5 segments in HPD. Such trees bring about the extreme case when naïve approaches are no longer feasible, whereas HPD-based solutions are at their best.)

Naïve structures $\text{nv}/\text{nv}^L/\text{nv}^c$ are visibly slower in PM than in PC, although both queries are resolved by explicitly traversing the path. This is expected, as for median, we first collect the nodes encountered into a vector, and then call a standard selection algorithm over it. In PC, by contrast, neither inserting into a container nor a subsequent search for median is involved. Succinct nv^c is about 10 times slower than the uncompressed counterpart, nv . The nv^L being little less than twice faster than its *LCA*-devoid counterpart, nv , is explained by the fact that the latter effectively traverses the query path twice – once to locate the *LCA*, and one more time to answer the query proper.

4.4 Path Counting Queries

Naïve structures $\text{nv}/\text{nv}^L/\text{nv}^c$ are insensitive to the change in κ , as indeed resolving a query on them is nothing but scanning the path along with incrementing an integer counter. For that matter, running times for `small` are slightly larger than those for `large`, but obviously this is attributed to fluctuations in the path-part of the query.

Succinct structures $\text{whp}^p/\text{whp}^c$ and $\text{ext}^p/\text{ext}^c$ feature decreasing running times as one moves from `large` to `small` – as the query weight-range shrinks, the chance of branching during the traversal of the implicit range tree decreases also. The fastest (uncompressed) whp^p and the slowest (compressed) ext^c succinct solutions differ by a factor of 4, which is intrinsically larger constants in ext^c ’s implementation compounded with slower `rank`/`select` primitives in compressed bitmaps at play. The slowest succinct, ext^c , is nonetheless competitive with the nv/nv^L in `large` setup, with the advantage of being independent of the tree diameter.

In ext^\dagger - whp^\dagger pair, the latter is usually 2-3 times slower, as one would expect, as, in addition to the inherent $\lg n$ -factor slowdown in whp^\dagger , following a pointer “downwards” (i.e. either determining 0/1-view in ext^\dagger and $\text{rank}_{0/1}()$ in whp^\dagger) each require one memory access.

4.5 Path Reporting Queries

Succinct structures $\text{whp}^p/\text{whp}^c$ and $\text{ext}^p/\text{ext}^c$ recover each reported node’s weight in $\mathcal{O}(\lg \sigma)$ time. One implication is, when $\lg n \ll \kappa$, the query time is dominated by $\mathcal{O}(\kappa \cdot \log \sigma)$, and whp - ext families perform comparably. A caveat regarding reporting queries is in order. It is clear from whp ’s design outlined in Section 3 that a path reporting query returns an original weight along with the *position in the permuted array C* – not the original preorder identifier of the node, as the ext does. (Design

Dataset	κ	nv	nv^L	ext^\dagger	whp^\dagger	nv^c	ext^c	ext^p	whp^c	whp^p	
eu.mst.osm	9,840	356	256	184	70.7	3766	large	large	large	large	large
eu.mst.dmcs	9,163	309	224	147	66.8	3485					
eu.emst.dem	14,211	389	241	140	77.5	4926					
mrs.emst.dem	10,576	267	178	89.2	55.1	3668					
eu.mst.osm	1,093	322	222	43.7	28.8	3706	medium	medium	medium	medium	medium
eu.mst.dmcs	1,090	277	196	34.0	29.7	3434					
eu.emst.dem	1,464	354	206	32.1	20.1	4880					
mrs.emst.dem	1,392	250	151	22.1	15.6	3639					
eu.mst.osm	182	311	212	13.8	19.0	3685	1965	485	795	226	small
eu.mst.dmcs	236	271	193	13.2	21.0	3529	2518	632	1043	292	
eu.emst.dem	215	353	203	10.2	12.7	4873	1276	378	590	205	
mrs.emst.dem	117	242	145	8.88	9.57	3632	881	278	475	162	

Table 5 – Average time to answer a path reporting query, from a fixed set of 10^6 randomly generated path reporting queries, in microseconds. The queries are given in **large**, **medium**, and **small** configurations. Average output size for each group is given in column κ .

of whp , decouples weight-queries from the underlying tree, but necessitates additional steps and space for converting positions in the permuted array back to node ids; we however chose to faithfully represent the original whp of [73].)

Secondly, with non-negligible κ (as in the non-small configurations), these structures are not suitable for use in PR. We thus run the experiments for the succinct structures whp^p/whp^c and ext^p/ext^c for the **small** configuration only (bottom-right corner in Table 5). We observe that the succinct structures ext^p and whp^p are competitive with nv/nv^L , in **small** setting: informally, time saved in locating the nodes to report is used to uncompress the nodes’ weights (whereas in nv/nv^L the weights are explicit.) Between the succinct families ext and whp , clearly the latter is faster, as simple `select()` on a sequence as we go up the wavelet tree tend to have lower constant factors than the counterpart operation on trees (BP sequences).

Plain pointer-based structures whp and ext exhibit the same order of magnitude in query time, with the former being sometimes little more than 2 times faster on non-small setups. There are two reasons for this, which are somewhat intertwined. Firstly, whp^\dagger returns an index to the permuted array rather than original node id. (Converting to original id would need one additional memory access.) Secondly, in the implicit range tree during the $2d$ search in whp^\dagger , when the current range is totally contained within the query range, we start reporting the node weights by simply incrementing a counter – position in the wavelet-tree sequence. By contrast, on such occasions ext^\dagger iterates through the nodes being reported calling `parent()`-operation for the current node, which is one additional memory access compared to whp^\dagger . We again seem to confirm a (non-surprising) fact that operations on trees tend to be little more expensive than similar operations on sequences.

Naïve structures $nv/nv^L/nv^c$ are less sensitive to the query weight range’s magnitude, since they simply scan the path along with pushing into a container. The differences in running time in Table 5 between the configurations are thus accounted for by the cost of inserting into container (C++’s `std::vector`) in our realizations). Naïve structures’ running time for path reporting being dependent solely on the query path’s length, they become quickly unfeasible in the worst case of large diameters (whereas they may be suitable for shallow trees, such as e.g. trees originating from “small-world” networks).

XX:12 Path Query Data Structures

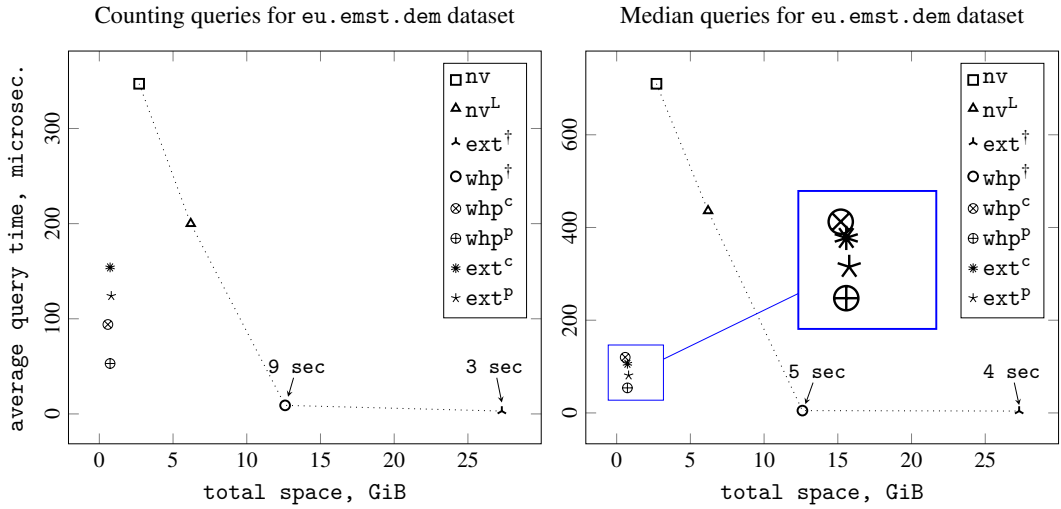


Fig. 3. Visualization of some of the entries in Table 4. Inner rectangle magnifies the mutual configuration of the succinct data structures whp^{P} , whp^{C} , ext^{P} , and ext^{C} . The succinct naïve structure nv^{C} is not shown.

5 Conclusion

We have designed and experimentally evaluated recent algorithmic proposals in path queries in weighted trees, by either faithfully replicating them or offering practical alternatives. Our data structures include both plain pointer-based and succinct implementations.

In a set of experiments on large practical datasets, we measure both query time and space performance of our data structures. We find that the succinct structures we implement offer an attractive alternative to plain pointer-based solutions, in scenarios with critical space occupancy, reasonable tolerance to slowdown, and optimal worst-case query time performance. Some of the structures we implement (whp^{C}) occupy space equal to bare compressed storage (nv^{C}) of the object and yet offer fast queries on top of it, while another structure ($\text{ext}^{\text{C}}/\text{ext}^{\text{P}}$) occupies space close to nv^{C} , offers fast queries, and has low peak memory for construction.

Implementation of the theoretically optimal, both in space and query time, solution to the path query types we have considered in this study, remains an interesting open problem in algorithm engineering.

References

- 1 DIMACS'09. <http://users.diag.uniroma1.it/challenge9/download.shtml>. Accessed: 07/12/2018.
- 2 Euclidean MST Example. https://doc.cgal.org/latest/BGL/BGL_triangulation_2_2emst_8cpp-example.html. Accessed: 10/01/2019.
- 3 googlebenchmark microbenchmarking library. <https://github.com/google/benchmark>. Accessed: 23/12/2019.
- 4 googletest unit testing library. <https://github.com/google/googletest>. Accessed: 23/12/2019.
- 5 KIT roadgraphs. <https://i11www.iti.kit.edu/information/roadgraphs>. Accessed: 07/12/2018.
- 6 ltree module for PostgreSQL RDBMS. <https://www.postgresql.org/docs/current/ltree.html>. Accessed: 10/01/2020.
- 7 malloc-count.

- 8 MOLA mars orbiter laser altimeter data from nasa mars global surveyor.
https://planetarymaps.usgs.gov/mosaic/Mars_MGS_MOLA_DEM_mosaic_global_463m.tif. Accessed: 10/01/2019.
- 9 OSM europe maps. <http://download.geofabrik.de/europe.html>. Accessed: 23/11/2018.
- 10 Postgis spatial and geographic objects for postgresql. <http://postgis.net/>. Accessed: 01/12/2018.
- 11 SRTM shuttle radar topography mission. <http://srtm.csi.cgiar.org/srtmdata/>. Accessed: 10/01/2019.
- 12 Stack Overflow thread on recursive queries.
<https://stackoverflow.com/questions/324935/mysql-with-clause>. Accessed: 31/08/2019.
- 13 Stanford Network Analysis Project. <https://snap.stanford.edu/index.html>. Accessed: 03/11/2018.
- 14 STL nth_element().
- 15 Andrés Abeliuk, Rodrigo Cánovas, and Gonzalo Navarro. Practical compressed suffix trees. *Algorithms*, 6(2):319–351, 2013. URL: <https://doi.org/10.3390/a6020319>, doi:10.3390/a6020319.
- 16 Ravindra K. Ahuja, Thomas L. Magnanti, and James B. Orlin. *Network flows - theory, algorithms and applications*. Prentice Hall, 1993.
- 17 Noga Alon and Baruch Schieber. Optimal preprocessing for answering on-line product queries. Technical report, Tel-Aviv University, 1987.
- 18 Diego Arroyuelo, Rodrigo Cánovas, Gonzalo Navarro, and Kunihiko Sadakane. Succinct trees in practice. In *Proceedings of the Twelfth Workshop on Algorithm Engineering and Experiments, ALENEX 2010, Austin, Texas, USA, January 16, 2010*, pages 84–97, 2010. URL:
<https://doi.org/10.1137/1.9781611972900.9>, doi:10.1137/1.9781611972900.9.
- 19 Diego Arroyuelo, Francisco Claude, Reza Dorrigiv, Stephane Durocher, Meng He, Alejandro López-Ortiz, J. Ian Munro, Patrick K. Nicholson, Alejandro Salinger, and Matthew Skala. Untangled monotonic chains and adaptive range search. *Theor. Comput. Sci.*, 412(32):4200–4211, 2011. URL:
<https://doi.org/10.1016/j.tcs.2011.01.037>, doi:10.1016/j.tcs.2011.01.037.
- 20 M. D. Atkinson and Jörg-Rüdiger Sack. Generating binary trees at random. *Inf. Process. Lett.*, 41(1):21–23, 1992. URL: [https://doi.org/10.1016/0020-0190\(92\)90075-7](https://doi.org/10.1016/0020-0190(92)90075-7), doi:10.1016/0020-0190(92)90075-7.
- 21 Lilian Beckert. personal communication.
- 22 Michael A. Bender, Martin Farach-Colton, Giridhar Pemmasani, Steven Skiena, and Pavel Sumazin. Lowest common ancestors in trees and directed acyclic graphs. *J. Algorithms*, 57(2):75–94, 2005. URL: <https://doi.org/10.1016/j.jalgor.2005.08.001>, doi:10.1016/j.jalgor.2005.08.001.
- 23 David Benoit, Erik D. Demaine, J. Ian Munro, Rajeev Raman, Venkatesh Raman, and S. Srinivasa Rao. Representing trees of higher degree. *Algorithmica*, 43(4):275–292, 2005. URL:
<https://doi.org/10.1007/s00453-004-1146-6>, doi:10.1007/s00453-004-1146-6.
- 24 Nieves R. Brisaboa, Guillermo de Bernardo, Roberto Konow, Gonzalo Navarro, and Diego Seco. Aggregated 2D range queries on clustered points. *Inf. Syst.*, 60:34–49, 2016. URL:
<https://doi.org/10.1016/j.is.2016.03.004>, doi:10.1016/j.is.2016.03.004.
- 25 Gerth Stølting Brodal, Beat Gfeller, Allan Grønlund Jørgensen, and Peter Sanders. Towards optimal range medians. *Theor. Comput. Sci.*, 412(24):2588–2601, 2011. URL:
<https://doi.org/10.1016/j.tcs.2010.05.003>, doi:10.1016/j.tcs.2010.05.003.
- 26 Valentin Buchhold. personal communication.
- 27 Joe Celko. *Joe Celko's Trees and Hierarchies in SQL for Smarties*. Morgan Kaufmann Publishers Inc., San Francisco, CA, USA, 2 edition, 2012.
- 28 Timothy M. Chan, Meng He, J. Ian Munro, and Gelin Zhou. Succinct indices for path minimum, with applications. *Algorithmica*, 78(2):453–491, 2017. URL:
<https://doi.org/10.1007/s00453-016-0170-7>, doi:10.1007/s00453-016-0170-7.
- 29 Timothy M. Chan, Kasper Green Larsen, and Mihai Patrascu. Orthogonal range searching on the ram, revisited. In *Computational Geometry, 27th ACM Symposium, SoCG 2011, Paris, France, June 13-15, 2011. Proceedings*, pages 1–10, 2011. URL: <https://doi.org/10.1145/1998196.1998198>, doi:10.1145/1998196.1998198.

XX:14 Path Query Data Structures

30 Bernard Chazelle. Computing on a free tree via complexity-preserving mappings. *Algorithmica*, 2(1):337–361, Nov 1987. URL: <https://doi.org/10.1007/BF01840366>, doi:10.1007/BF01840366.

31 Yi-Ting Chiang, Ching-Chi Lin, and Hsueh-I Lu. Orderly spanning trees with applications. *SIAM J. Comput.*, 34(4):924–945, 2005. URL: <https://doi.org/10.1137/S0097539702411381>, doi:10.1137/S0097539702411381.

32 Francisco Claude. libcds. <https://github.com/fclaude/libcds>. Accessed: 10/02/2018.

33 Francisco Claude, J. Ian Munro, and Patrick K. Nicholson. Range queries over untangled chains. In *String Processing and Information Retrieval - 17th International Symposium, SPIRE 2010, Los Cabos, Mexico, October 11-13, 2010. Proceedings*, pages 82–93, 2010. URL: https://doi.org/10.1007/978-3-642-16321-0_8, doi:10.1007/978-3-642-16321-0_8.

34 Thomas H. Cormen, Charles E. Leiserson, Ronald L. Rivest, and Clifford Stein. *Introduction to Algorithms*, 3rd Edition. MIT Press, 2009. URL: <http://mitpress.mit.edu/books/introduction-algorithms>.

35 O’Neil Delpratt, Naila Rahman, and Rajeev Raman. Engineering the LOUDS succinct tree representation. In *Experimental Algorithms, 5th International Workshop, WEA 2006, Cala Galdana, Menorca, Spain, May 24-27, 2006, Proceedings*, pages 134–145, 2006. URL: https://doi.org/10.1007/11764298_12, doi:10.1007/11764298_12.

36 Erik D. Demaine, Gad M. Landau, and Oren Weimann. On cartesian trees and range minimum queries. *Algorithmica*, 68(3):610–625, 2014. URL: <https://doi.org/10.1007/s00453-012-9683-x>, doi:10.1007/s00453-012-9683-x.

37 Arash Farzan and J. Ian Munro. A uniform paradigm to succinctly encode various families of trees. *Algorithmica*, 68(1):16–40, 2014. URL: <https://doi.org/10.1007/s00453-012-9664-0>, doi:10.1007/s00453-012-9664-0.

38 José Fuentes and Gonzalo Navarro. Experimental datasets graphs, trees, parentheses. <https://users.dcc.uchile.cl/~jfuentess/datasets/trees.php>. Accessed: 2018-03-14.

39 Travis Gagie, Simon J. Puglisi, and Andrew Turpin. Range quantile queries: Another virtue of wavelet trees. In *String Processing and Information Retrieval, 16th International Symposium, SPIRE 2009, Saariselkä, Finland, August 25-27, 2009, Proceedings*, pages 1–6, 2009. URL: https://doi.org/10.1007/978-3-642-03784-9_1, doi:10.1007/978-3-642-03784-9_1.

40 GDAL/OGR contributors. *GDAL/OGR Geospatial Data Abstraction software Library*. Open Source Geospatial Foundation, 2019. URL: <https://gdal.org>.

41 Richard F. Geary, Naila Rahman, Rajeev Raman, and Venkatesh Raman. A simple optimal representation for balanced parentheses. *Theor. Comput. Sci.*, 368(3):231–246, 2006. URL: <https://doi.org/10.1016/j.tcs.2006.09.014>, doi:10.1016/j.tcs.2006.09.014.

42 Richard F. Geary, Rajeev Raman, and Venkatesh Raman. Succinct ordinal trees with level-ancestor queries. *ACM Trans. Algorithms*, 2(4):510–534, 2006. URL: <https://doi.org/10.1145/1198513.1198516>, doi:10.1145/1198513.1198516.

43 Simon Gog. SDSL cheatsheet. <http://simongog.github.io/assets/data/sdsl-cheatsheet.pdf>.

44 Simon Gog, Timo Beller, Alistair Moffat, and Matthias Petri. From theory to practice: Plug and play with succinct data structures. In *Experimental Algorithms - 13th International Symposium, SEA 2014, Copenhagen, Denmark, June 29 - July 1, 2014. Proceedings*, pages 326–337, 2014. URL: https://doi.org/10.1007/978-3-319-07959-2_28, doi:10.1007/978-3-319-07959-2_28.

45 Roberto Grossi and Giuseppe Ottaviano. Design of practical succinct data structures for large data collections. In *Experimental Algorithms, 12th International Symposium, SEA 2013, Rome, Italy, June 5-7, 2013. Proceedings*, pages 5–17, 2013. URL: https://doi.org/10.1007/978-3-642-38527-8_3, doi:10.1007/978-3-642-38527-8_3.

46 Torben Hagerup. Parallel preprocessing for path queries without concurrent reading. *Inf. Comput.*, 158(1):18–28, 2000. URL: <https://doi.org/10.1006/inco.1999.2814>, doi:10.1006/inco.1999.2814.

47 Meng He and Serikzhan Kazi. Path and ancestor queries over trees with multidimensional weight vectors. In *30th International Symposium on Algorithms and Computation, ISAAC 2019, December 8-11, 2019, Shanghai University of Finance and Economics, Shanghai, China*, pages 45:1–45:17, 2019. URL: <https://doi.org/10.4230/LIPIcs.ISAAC.2019.45>, doi:10.4230/LIPIcs.ISAAC.2019.45.

48 Meng He, J. Ian Munro, and Srinivasa Rao Satti. Succinct ordinal trees based on tree covering. *ACM Trans. Algorithms*, 8(4):42:1–42:32, 2012. URL: <https://doi.org/10.1145/2344422.2344432>, doi:10.1145/2344422.2344432.

49 Meng He, J. Ian Munro, and Gelin Zhou. Path queries in weighted trees. In *Algorithms and Computation - 22nd International Symposium, ISAAC 2011, Yokohama, Japan, December 5-8, 2011. Proceedings*, pages 140–149, 2011. URL: https://doi.org/10.1007/978-3-642-25591-5_16, doi:10.1007/978-3-642-25591-5\16.

50 Meng He, J. Ian Munro, and Gelin Zhou. A framework for succinct labeled ordinal trees over large alphabets. *Algorithmica*, 70(4):696–717, 2014. URL: <https://doi.org/10.1007/s00453-014-9894-4>, doi:10.1007/s00453-014-9894-4.

51 Meng He, J. Ian Munro, and Gelin Zhou. Data structures for path queries. *ACM Trans. Algorithms*, 12(4):53:1–53:32, 2016. URL: <https://doi.org/10.1145/2905368>, doi:10.1145/2905368.

52 Kazuki Ishiyama and Kunihiko Sadakane. A succinct data structure for multidimensional orthogonal range searching. In *2017 Data Compression Conference, DCC 2017, Snowbird, UT, USA, April 4-7, 2017*, pages 270–279, 2017. URL: <https://doi.org/10.1109/DCC.2017.47>, doi:10.1109/DCC.2017.47.

53 Guy Jacobson. Space-efficient static trees and graphs. In *30th Annual Symposium on Foundations of Computer Science, Research Triangle Park, North Carolina, USA, 30 October - 1 November 1989*, pages 549–554, 1989. URL: <https://doi.org/10.1109/SFCS.1989.63533>, doi:10.1109/SFCS.1989.63533.

54 Joseph JáJá, Christian Worm Mortensen, and Qingmin Shi. Space-efficient and fast algorithms for multidimensional dominance reporting and counting. In *Algorithms and Computation, 15th International Symposium, ISAAC 2004, Hong Kong, China, December 20-22, 2004. Proceedings*, pages 558–568, 2004. URL: https://doi.org/10.1007/978-3-540-30551-4_49, doi:10.1007/978-3-540-30551-4\49.

55 Jesper Jansson, Kunihiko Sadakane, and Wing-Kin Sung. Ultrasuccinct representation of ordered trees with applications. *J. Comput. Syst. Sci.*, 78(2):619–631, 2012. URL: <https://doi.org/10.1016/j.jcss.2011.09.002>, doi:10.1016/j.jcss.2011.09.002.

56 Donald Ervin Knuth. *The art of computer programming, Volume II: Seminumerical Algorithms*, 3rd Edition. Addison-Wesley, 1998. URL: <http://www.worldcat.org/oclc/312898417>.

57 Danny Krizanc, Pat Morin, and Michiel H. M. Smid. Range mode and range median queries on lists and trees. *Nord. J. Comput.*, 12(1):1–17, 2005.

58 Hsueh-I Lu and Chia-Chi Yeh. Balanced parentheses strike back. *ACM Trans. Algorithms*, 4(3):28:1–28:13, 2008. URL: <https://doi.org/10.1145/1367064.1367068>, doi:10.1145/1367064.1367068.

59 Erkki Mäkinen. Generating random binary trees – a survey. Technical report, University of Tampere, 1998.

60 Carsten Moeller. OSMPO converter and routing engine. <http://osm2po.de>. Accessed: 01/12/2018.

61 J. Ian Munro, Rajeev Raman, Venkatesh Raman, and S. Srinivasa Rao. Succinct representations of permutations and functions. *Theor. Comput. Sci.*, 438:74–88, 2012. URL: <https://doi.org/10.1016/j.tcs.2012.03.005>, doi:10.1016/j.tcs.2012.03.005.

62 J. Ian Munro and Venkatesh Raman. Succinct representation of balanced parentheses and static trees. *SIAM J. Comput.*, 31(3):762–776, 2001. URL: <https://doi.org/10.1137/S0097539799364092>, doi:10.1137/S0097539799364092.

63 David R. Musser. Introspective sorting and selection algorithms. *Softw., Pract. Exper.*, 27(8):983–993, 1997.

64 Gonzalo Navarro. Wavelet trees for all. *J. Discrete Algorithms*, 25:2–20, 2014. URL: <https://doi.org/10.1016/j.jda.2013.07.004>, doi:10.1016/j.jda.2013.07.004.

XX:16 Path Query Data Structures

65 Gonzalo Navarro. *Compact Data Structures - A Practical Approach*. Cambridge University Press, 2016.
URL: <http://www.cambridge.org/de/academic/subjects/computer-science/algoritmics-complexity-computer-algebra-and-computational-g/compact-data-structures-practical-approach?format=HB>.

66 Gonzalo Navarro and Alberto Ordóñez Pereira. Faster compressed suffix trees for repetitive collections. *ACM Journal of Experimental Algorithmics*, 21(1):1.8:1–1.8:38, 2016. URL: <https://doi.org/10.1145/2851495>, doi:10.1145/2851495.

67 Gonzalo Navarro and Eliana Providel. Fast, small, simple rank/select on bitmaps. In *Experimental Algorithms - 11th International Symposium, SEA 2012, Bordeaux, France, June 7-9, 2012. Proceedings*, pages 295–306, 2012. URL: https://doi.org/10.1007/978-3-642-30850-5_26, doi:10.1007/978-3-642-30850-5_26.

68 Yakov Nekrich. A data structure for multi-dimensional range reporting. In *Computational Geometry, 23rd ACM Symposium, SoCG 2007, Gyeongju, South Korea, June 6-8, 2007. Proceedings*, pages 344–353, 2007. URL: <https://doi.org/10.1145/1247069.1247130>, doi:10.1145/1247069.1247130.

69 Yakov Nekrich and Gonzalo Navarro. Sorted range reporting. In *Algorithm Theory, 13th Scandinavian Symposium and Workshops, SWAT 2012, Helsinki, Finland, July 4-6, 2012. Proceedings*, pages 271–282, 2012. URL: https://doi.org/10.1007/978-3-642-31155-0_24, doi:10.1007/978-3-642-31155-0_24.

70 Alber Nijenhuis and Herbert S. Wilf. *Combinatorial Algorithms*. Academic Press, 1978.

71 OpenStreetMap contributors. Planet dump retrieved from <https://planet.osm.org> .
<https://www.openstreetmap.org>, 2017.

72 Giuseppe Ottaviano. succinct. <https://github.com/ot/succinct>. Accessed: 10/02/2018.

73 Manish Patil, Rahul Shah, and Sharma V. Thankachan. Succinct representations of weighted trees supporting path queries. *J. Discrete Algorithms*, 17:103–108, 2012. URL: <https://doi.org/10.1016/j.jda.2012.08.003>, doi:10.1016/j.jda.2012.08.003.

74 Nicola Prezza. Dynamic. <https://github.com/xxsds/DYNAMIC>.

75 Nicola Prezza. A framework of dynamic data structures for string processing. In *16th International Symposium on Experimental Algorithms, SEA 2017, June 21-23, 2017, London, UK*, pages 11:1–11:15, 2017. URL: <https://doi.org/10.4230/LIPIcs.SEA.2017.11>, doi:10.4230/LIPIcs.SEA.2017.11.

76 A. Rényi and G. Szekeres. On the height of trees. *Journal of the Australian Mathematical Society*, 7(4):497–507, 1967.

77 Kunihiko Sadakane. Compressed suffix trees with full functionality. *Theory Comput. Syst.*, 41(4):589–607, 2007. URL: <https://doi.org/10.1007/s00224-006-1198-x>, doi:10.1007/s00224-006-1198-x.

78 Daniel D. Sleator and Robert Endre Tarjan. A data structure for dynamic trees. *J. Comput. Syst. Sci.*, 26(3):362–391, June 1983. URL: [http://dx.doi.org/10.1016/0022-0000\(83\)90006-5](http://dx.doi.org/10.1016/0022-0000(83)90006-5), doi:10.1016/0022-0000(83)90006-5.

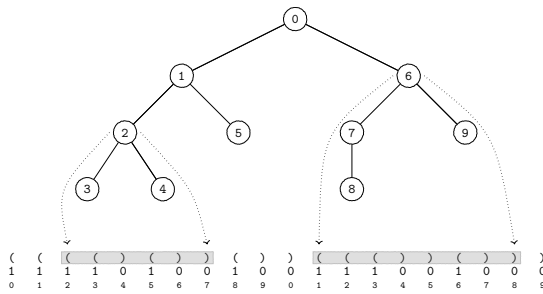
79 The CGAL Project. *CGAL User and Reference Manual*. CGAL Editorial Board, 4.14 edition, 2019. URL: <https://doc.cgal.org/4.14/Manual/packages.html>.

80 Sebastiano Vigna. Sux. <http://sux.di.unimi.it/>. Accessed: 13/02/2018.

81 Herbert S. Wilf. The uniform selection of free trees. *J. Algorithms*, 2(2):204–207, 1981. URL: [https://doi.org/10.1016/0196-6774\(81\)90021-3](https://doi.org/10.1016/0196-6774(81)90021-3), doi:10.1016/0196-6774(81)90021-3.

A Balanced Parentheses and Ordinal Trees

Balanced parentheses (BP) is a way of linearising the tree by emitting "(" upon first entering a node and ")" upon exiting, having explored all its descendants during the preorder traversal of the tree. To develop intuition, we refer to Figure 4.



■ **Fig. 4.** An ordinal tree, preorder labeled. Sequences: (top) Balanced parentheses sequence BP; (middle) bitvector, representing BP; (bottom) positions. In BP, "(" is 1. Arrows point to the opening and closing parentheses corresponding to the node. Shadings mark subtrees.

It is clear, for example, that a subtree rooted at a particular node u is encoded in a portion between the parentheses-pair (say, at positions i and j) corresponding to u . It follows that a node u is an ancestor of a node v if and only if the interval of the former encloses the interval of the latter; the corresponding primitive is `is_ancestor()`. For these i and j , a call to `is_opening(i)` returns TRUE, whereas `is_opening(j)` is FALSE. Also, it is clear that the preorder number of a vertex is the number of times a "(" occurs before the opening parenthesis of u , or, in the above terms, `rank1(S, i)`. Furthermore, for a closing parenthesis at j a primitive `find_open()` is defined to return i ; and `enclose(i)` returns the opening position of the tightest pair enclosing i and j . Now, finding the *LCA* of two nodes would be equivalent to enclosing both of the opening parentheses corresponding to these nodes by the tightest pair of matching parentheses. Technically, a BP is an ordinary bitmap, with an opening parenthesis encoded as 1, and the closing parenthesis encoded as 0. Since we identify nodes with their preorder numbers, we move back and forth between a node and its opening parenthesis using `pos2node()` and `node2pos()` wrappers around the corresponding `rank` and `select` calls, as in `node2pos(x) = select1(BPS, x + 1)`, `pos2node(i) = rank1(BPS, i)`. This infrastructure effectively melds nodes with its opening/closing parenthesis position.

B Implementation Details

Engineering data structures that occupy space asymptotically close to the information-theoretic minimum, yet efficiently support non-trivial queries, is a challenging task that is only made possible by groundwork laid by the community of researchers and practitioners, whose collective effort resulted in comprehensive codebase [67, 45, 44, 75], among which are `succinct` [72] by Ottaviano, `libcds` [32] by Claude, `DYNAMIC` [74] by Prezza (all in C++), `Sux` [80] by Vigna (in Java), and a somewhat more restricted in scope `rsdic` by Navarro and Providel [67]. Provided are core primitives, such as bitmaps, rank/select, and balanced parentheses support, to build more complex structures out of them. One of the most mature `succinct` data structures library at the moment of writing is that of Gog et al. [44], which is our tool of choice.

Plain pointer-based structures rely on STL components only. Standard `std::nth_element()` function [14] is used as the selection algorithm in PM.

Succinct structures `extP`, `extC`, `whpP`, and `whpC` are implemented as template classes parameterized with bitmap-type, rank/select, and BP-support structures. An arbitrary combination of bitmaps and rank/select indices is not necessarily compatible [43]. We thus focus on two bitmap types: a compressed bitmap (`sds1::rrr_vector`) and plain bitmap (`sds1::bit_vector`). Whenever applicable, we also use the integer-vector class `sds1::int_vector<>`, which accepts bit-width as template parameter, instead of `std::vector<int>` of STL. Thus, for nv^c , the weights are stored using $\lg \sigma$ bits each, and the structure theoretically occupies $2n + n \lg \sigma + \mathcal{O}(n \lg \sigma)$ bits. For uniformity, across

our data structures, tree navigation is provided solely by `sds1::bp_support_gg` BP-support class, chosen on the basis of our benchmarks on a large random tree. We extended `sds1::wt_int` with a range quantile searching function, and optimized, for PC/PR, `sds1::wt_int`'s own $2d$ -range searching method; for the `whp` structure, this led to a significant improvement (tens of times faster) in speed, compared to the library version.

Plain pointer-based implementation ext^\dagger conceptually is an uncompressed $\text{ext}^p/\text{ext}^c$. The sequence of original weights is stored explicitly, and for each tree T that arises in the recursive process, at each node $x \in T$, we precompute and store the node's parent in T , views $x_0 \in T_0, x_1 \in T_1$, and the node's depth in T . The outermost tree is preprocessed for an *LCA*-support structure of [22]. The items of whp^\dagger and ext^\dagger both store, at each level, the pointer to the original node, to recover the weight in constant time.

C Datasets

C.1 Generating Trees Uniformly at Random

There are methods for generating free trees [81] or rooted unlabeled ordinal trees uniformly at random (u.a.r.) (see [59] for a relevant survey). An algorithm of [70] is elegant and simple, but impractical: the calculations are performed with the actual number of trees t_n , which is exponential in n . Short of arbitrary-precision types such as e.g. the ones provided by Java's `BigDecimal/BigInteger` classes, which would add non-negligible time/space overhead into the bargain, this is not a practical option. Since generating random ordinal trees is equivalent to generating random balanced parentheses sequences, we used the algorithm of [20] instead, which, in contrast, operates with numbers that are at most $2n$, i.e. that fit into standard integer types of C++. The algorithm proceeds by an assignment of n opening parentheses into $2n$ slots using a random subset generation of [56], with the subsequent "correction" of the resulting parenthesis sequence to be a valid one. The justification is in a certain bijection between the set of balanced parentheses sequences and parentheses sequences with the fixed number of "defects" (see [20] for details.)

C.2 Practical Datasets

In this section, described is the pipeline for data preprocessing for the real-world datasets used in our study.

OpenStreetMap (OSM) dataset `eu.mst.osm` originates from *Open Street Map* (OSM) project [71]. We converted OSM data from [9] to `*.sql` insert-files using the well-known tool [60]. Our instance of PostgreSQL RDBMS, extended with Postgis [10], was then populated with the INSERTs obtained using `osm2po`, thereby making the OSM data *routable*. Finally, a simple SQL-query extracts all possible links as `source target km` triples format into a regular `*.csv` file.³ Thus, each line in our final file states that there is a road from `source` to `target` of length `km` kilometers, where the former two are some entities internal to OSM, and mere integer IDs for all practical purposes.

Next, we find a largest-cardinality minimum spanning tree (MST), for simplicity considering the graph to be bidirectional. We then orient the tree via a depth-first-search from a randomly selected but fixed source. The nodes are then assigned the (truncated) weights of the incoming arcs (with the source being assigned zero).

DIMACS dataset `eu.mst.dimcs` is from the 9th DIMACS challenge [1], and was obtained from [5]. The graph was converted from the raw DIMACS format, keeping only the largest strongly-

³ there are other ways of accomplishing this, e.g. via pgRouting at <http://pgrouting.org/>

connected component and removing multi-arcs. For `eu.mst.dmcs`, the metric is travel distance, in meters [21, 26]. The tree for `eu.mst.dmcs` was obtained in the way exactly similar to the `eu.mst.osm` dataset.

Digital Elevation Models (DEM) model lends itself to weighted-tree conversion rather naturally, with the (x, y) coordinates supplying the basis for tree topology (via e.g. Euclidean minimum spanning trees), and the elevation z serving as the weight. These datasets represent elevations above certain levels on a planet's surface (`eu.emst.dem`, `mrs.emst.dem`) and are each a result of the following two-phase procedure.

We outline the procedure for the first dataset, as the procedures for the latter is analogous.

The preprocessing phase fetches original raw data from [11], as 30-by-30 degree GeoTIFF tiles. Then the tiles are projected into Cartesian plane, in *Transverse Mercator projection* using meters, by issuing

```
gdalwarp -s_srs '+init=epsg:4326' -t_srs '+proj=tmerc +lat_0=44.00 +lon_0=15.00 +units=m'
```

via the `gdalwarp` tool of the *GDAL Geospatial Data Abstraction software Library* [40]. The exact command is

```
gdalwarp -s_srs '+init=epsg:4326' -t_srs '+proj=tmerc +lat_0=44.00 +lon_0=15.00 +units=m'
```

The projection is further dumped into the *XYZ* format via `gdal_translate` tool from GDAL, issuing

```
gdal\translate -of XYZ
```

What is referred to as “File in *XYZ* format” is essentially a collection of rows, containing x , y , and z values, being respectively the xy -coordinates of the projection along the (original) elevation of the projected point. Finally, the `nodata`-values concomitant to a projection were removed with UNIX’s standard `sed` tool, using e.g. a command

```
cat europe.xyz | sed '/\s\+-32768$/d' > europe_curated.xyz
```

The second phase constructs the *Euclidean minimum spanning tree* (EMST) using the *XYZ*-data obtained during phase one. We used *The Computational Geometry Algorithms Library* [79]; namely, we trivially adapted the example at [2]. The Mars Elevation (`mrs.emst.dem`) was obtained from [8] and processed similarly. Prior to building EMST, `eu.emst.dem` and `mrs.emst.dem` datasets were sampled u.a.r. to have the sizes shown in Table 2. In the case of `mrs.emst.dem`, the data has already been supplied in the *XYZ*-form, hence projection and translation steps do not apply.

D Query Algorithms

Range quantile queries over a collection of ranges proceeds as follows, with the lines referring to Algorithm 2.

Let us denote this set of intervals obtained as $I_m = \{[l_i, r_i]\}_{i=1}^m$. The range quantile algorithm of [39] is then generalized onto I_m as follows. We descend down the wavelet tree W_C maintaining a set of current weights $[a, b]$ (initially set to $[\sigma]$), the current node v initially set to root of the W_C , and the set of intervals I_m over C . When querying the current node v of the wavelet tree W_C with an interval $[l_j, r_j] \in I_m$, one finds out, in constant time, how many weights in the interval are lighter than the mid-point c of the current weight-set $[a, b]$, and how many of them are heavier (lines 6-7). Summing these respective values over all intervals (lines 5-7), we determine which subtree of the wavelet tree to descend to (line 9). Clearly, we need to update the intervals of the sequence I_m accordingly before the descent (lines 11-12) and lines 15-16). Path counting/reporting queries proceed by querying each interval, independently of the others, with the standard $2d$ search over wavelet trees.

Query algorithms in the ext data structure proceed in accordance with the generic approach, where we recurse on T_0 if $k < m$, for a query that asks for a node with the k -th smallest weight on the

XX:20 Path Query Data Structures

■ **Algorithm 2** – Range quantile: k -th smallest weight in $I_m = \bigcup_{i=1}^m [l_i, r_i]$

```

function RANGEQUANTILE( $v, k, I_m, [a, b]$ )
    if  $a == b$  then
        return  $a$ 
    3:     $acc_0, acc_1 \leftarrow 0, 0$ 
    for  $i \in [m]$  do
        6:         $acc_0 \leftarrow acc_0 + rank_0(r_i) - rank_0(l_i - 1)$ 
         $acc_1 \leftarrow acc_1 + rank_1(r_i) - rank_1(l_i - 1)$ 
         $c \leftarrow (a + b) / 2$ 
    9:    if  $acc_0 > k$  then
        for  $i \in [m]$  do
             $prefix \leftarrow rank_0(l_i - 1)$ 
        12:        $[l_i, r_i] \leftarrow [prefix + 1, rank_0(r_i + 1) - prefix]$ 
        return RANGEQUANTILE( $v_0, k, I_m, [a, c]$ )
        for  $i \in [m]$  do
        15:        $prefix \leftarrow rank_1(l_i - 1)$ 
             $[l_i, r_i] \leftarrow [prefix + 1, rank_1(r_i + 1) - prefix]$ 
        return RANGEQUANTILE( $v_1, k - acc_0, I_m, [c + 1, b]$ )

```

path between u_0 and v_0 ; otherwise, we recurse on T_1 with $k \leftarrow k - m$ and u_1, v_1 . We stop when a tree with homogeneous weights is encountered. This logic is embodied in Algorithm 3.

We enter Algorithm 3 with several parameters – the current tree T , the query nodes u, v , the *LCA* z of the two nodes, the quantile k we are looking for, the weight-range $[a, b]$, and a number w . These are initially set, respectively, to be the outermost tree, the original query nodes, the *LCA* of the original query nodes, the median’s index (i.e. half the length of the corresponding path in the original tree), the weight range $[\sigma]$, and the weight of the *LCA* of the original nodes. We maintain the invariant that T is weighted over $[a, b]$, z is the *LCA* of u and v in T . Line 2 checks whether the current tree is weight-homogeneous. If it is, we immediately return the current weight a (line 3). Otherwise, the quantile value we are looking for is either on the left or on the right half of the weight-range $[a, b]$. In lines 5-5 we check, successively, the ranges $[a_0, b_0]$ and $[a_1, b_1]$ to determine how many nodes on the path from u to v in T have weights from the corresponding interval. The accumulator variable acc keeps track of these values and is certain to always be at most k . When the next value of acc is about to become larger than k (line 11), we are certain that the current weight-interval is the one we should descend to (line 12). The invariants are maintained in line 6: there, we calculate the views of the current nodes u, v , and z in the extracted tree we are looking at.

It is clear that $\mathcal{O}(\lg \sigma)$ levels of recursion are explored. At each level of recursion, a constant number of `view_of()` and `depth()` operations are performed (lines 6-7). Hence, assuming the $\mathcal{O}(1)$ -time for the latter operations themselves, we have a $\mathcal{O}(\lg \sigma)$ query-time algorithm, overall.

A procedure for the path counting and reporting problems is essentially similar to that for the path median problem. We maintain two nodes, u and v , as the query nodes with respect to the current extraction T , and a node z as the lowest common ancestor of u and v in the current tree T . Initially, $u, v \in T$ are the original query nodes, and T is the outermost tree. Correspondingly, z is the *LCA* of the nodes u and v in the original tree; we determine the weight of z and store it in a constant variable w , which will be being passed down the recursion. Let $[a, b]$ be the query interval, and $[p, q]$ be the current range of weights of the tree. Initially, $[p, q] = [\sigma]$. Upon entering the procedure, we check whether the current interval $[p, q]$ lies entirely within the query interval $[a, b]$. If so, the entire path $A_{u,z} \cup A_{v,z}$ belongs to the answer. Here, we also check whether $w \in [a, b]$. Then we recurse on the

■ **Algorithm 3** – Selection: return the k -th smallest weight on the path from $u \in T$ to $v \in T$

Require: $z = LCA(u, v)$, $a \leq b$, $k \geq 0$

```

function SELECT( $T, u, v, z, k, w, [a..b]$ )
  if  $a == b$  then
    return  $a$ 
  3:    $acc \leftarrow 0$ 
  for  $t \in 0..1$  do
  6:      $iu, iv, iz \leftarrow view\_of(u, t), view\_of(v, t), view\_of(z, t)$ 
         $du, dv, dz \leftarrow depth(B_t, ix), depth(B_t, iy), depth(B_t, iz)$ 
         $dw \leftarrow du + dv - 2 \cdot dz$ 
  9:     if  $a_t \leq w \leq b_t$  then            $\triangleright [a_0..b_0] = [a..m], [a_1..b_1] = [m + 1..b], m = (a + b)/2$ 
         $dw \leftarrow dw + 1$ 
     11:    if  $acc + dw > k$  then
        12:      return SELECT( $T_t, iu, iv, iz, k - acc, w, [a_t..b_t]$ )
         $acc \leftarrow acc + dw$ 
  13:    assert(false);            $\triangleright$  unreachable statement – line 12 should execute at some point

```

trees T_t ($t \in \{0, 1\}$) having computed the corresponding T_t -views of the nodes u, v , and z , and with the corresponding current range.

Algorithm 4 is adapted from [51], and reasoning similar to Algorithm 3 applies. Now we have a weight-range parameter $[p, q]$, and we maintain that $[p, q] \cap [a, b] \neq \emptyset$ (the appropriate check is in line 11). In line 2 we check if the query range $[p, q]$ is completely inside the the current range. If so, we return all the nodes (if *report* argument is set to TRUE) and the number thereof (for counting case). If not, we descend to T_0 and T_1 (line 14), as discussed previously.

■ **Algorithm 4** – Counting and reporting.

Require: $z = LCA(u, v)$, $p \leq q$

```

function COUNTREPORT( $T, u, v, z, w, [p, q], [a, b], \text{vec} = \text{null}, \text{report} = \text{False}$ )
    if  $p \leq a \leq b \leq q$  then
        3:       if  $\text{report}$  then
            for  $\text{pu} \in \mathcal{A}(u)$  and  $\text{pu} \neq z$  do
                 $\text{vec} \leftarrow \text{vec} + \text{original\_node}(\text{pu})$ 
            6:       for  $\text{pv} \in \mathcal{A}(v)$  and  $\text{pv} \neq z$  do
                 $\text{vec} \leftarrow \text{vec} + \text{original\_node}(\text{pv})$ 
                if  $a \leq w \leq b$  then
                    9:            $\text{vec} \leftarrow \text{vec} + \text{original\_node}(\text{pv})$ 
                return  $\text{depth}(u) + \text{depth}(v) - 2\text{depth}(z) + 1_{w \in [p, q]}$ 
                if  $[p, q] \cap [a, b] = \emptyset$  then
                    12:           return 0
                     $\text{res} \leftarrow 0$ 
                    for  $t \in 0..1$  do            $\triangleright [a_0, b_0] = [a, m], [a_1, b_1] = [m + 1, b], m = (a + b)/2$ 
                    15:            $\text{iu}, \text{iv}, \text{iz} \leftarrow \text{view\_of}(u, t), \text{view\_of}(v, t), \text{view\_of}(z, t)$ 
                         $\text{du}, \text{dv}, \text{dz} \leftarrow \text{depth}(\text{B}_t, \text{ix}), \text{depth}(\text{B}_t, \text{iy}), \text{depth}(\text{B}_t, \text{iz})$ 
                         $\text{res} \leftarrow \text{res} + \text{COUNTREPORT}(T_t, \text{iu}, \text{iv}, \text{iz}, w, [p, q], [a_t, b_t], \text{vec}, \text{report})$ 
                18:           return  $\text{res}$ 

```
